Ordering of clusters during late-stage growth on surfaces

G. R. Carlow, R. J. Barel, and M. Zinke-Allmang
Department of Physics and Astronomy, The University of Western Ontario, London, Ontario, Canada N6A 3K7
(Received 21 January 1997; revised manuscript received 3 June 1997)

The size ordering and spatial ordering of metal clusters on semiconductor surfaces has been experimentally investigated for systems in the late stages of phase separation. Specific late stage cluster growth mechanisms were achieved by suitable experimental conditions, and include (i) Ostwald ripening, (ii) coalescence, and (iii) an ''intermediate'' regime where mass conservation is only marginally violated by a relatively small deposition rate during cluster growth. The size ordering and spatial ordering of clusters were quantified by the standard deviations of the cluster size distribution and the nearest-neighbor distribution, respectively. In the Ostwald ripening regime, the size distribution is less ordered (broader) and the spatial distribution is more ordered (narrower) than is predicted by the mean-field Lifshitz-Slyozov ripening theory. In the intermediate regime, a higher degree of size ordering is observed (when compared to Ostwald ripening), but little spatial ordering with a near random spatial distribution. Finally, in the coalescence regime little size ordering and no spatial ordering are observed. These results are described using a model of local ripening, a mechanism where the ripening of an individual cluster is dominated by its nearest neighbor rather than the global growth conditions. [S0163-1829(97)00944-2]

INTRODUCTION

Several methods to create spatially ordered structures on surfaces without using lithographic methods (self-assembling structures) have been studied recently in hopes to overcome major technological limitations in the growth of structures which allow us to implement quantum-confinement effects in semiconductor device designs.[1] While all these cases exploit specific properties of the used materials systems, the need of a surface phase-separation process during formation of the self-assembling structures is a common requirement.

Of underlying fundamental interest is therefore the degree of ordering that is obtainable with the isolated phase-separation processes alone, i.e., under exclusion of strong cluster-substrate interactions, substrate prepatterning, e.g., with the step bunching, or other concurring processes which introduce specific material-dependent parameters and limit thus the generality of the conclusions.

In the present study, we have chosen systems which show clustering under these conditions. The study focuses on the dominant late stage phase-separation processes, as these depend the least on details of the substrate structure.[2] We have studied the entire range of processes observable as a function of deposition rate, as this parameter allows us consistently to proceed from ripening dominated growth (mass-conserved systems) to coalescence-dominated growth (nonmass-conserved case). A transition between both regimes has been included where the deposition rate is smaller than diffusive mass transfer between clusters.[2] For ripening growth we will compare our data with the well-known models for the Ostwald ripening based on the quantitative treatments of Lifshitz and Slyozov[3] and Chakraverty.[4]

EXPERIMENTAL DETAILS

Experiments were performed under ultrahigh vacuum conditions in a molecular-beam epitaxy facility at the University of Western Ontario. The growth chamber is equipped with three standard effusion cells charged with Ga, Sn, and In, a shutter for each source, and a heated sample stage. The base pressure in the growth chamber was less than 5×10^{-10} Torr. Prior to insertion in the growth system, *ex situ* chemical treatment of Si(111) (Ref. 5) and GaAs(001) (Ref. 6) substrates was done to grow protective oxides. These oxides were subsequently flashed off in the growth chamber at elevated temperatures (850 °C for Si and 600 °C for GaAs) resulting in clean starting surfaces prior to metal deposition. Growth of metal clusters on the clean substrates was accomplished by metal deposition in combination with substrate annealing. Specific conditions are chosen which reproducibly result in specific growth mechanisms (Ostwald ripening or coalescence[2]).

We explore three sets of conditions.

(1) *Coalescence-dominated growth* was obtained by annealing of GaAs(001) substrates at 660 °C. The continual addition of Ga to the surface, caused by the preferential loss of As_2 at these annealing temperatures,[6] results in Ga cluster morphologies which are consistent with coalescence-dominated growth.[7]

(2) *Ostwald ripening dominated growth* was obtained by metal deposition (Sn or In) on room-temperature Si(111) substrates followed by post-deposit annealing at temperatures below metal desorption or bulk in-diffusion temperatures, i.e., the amount of material on the surface was conserved during clustering.

(3) An *intermediate regime* establishing conditions in between Ostwald ripening and coalescence, for the system Sn/Si(111). This was obtained by continual Sn deposition during substrate annealing, so that clusters grow in the presence of an external flux. The Sn deposition rate was sufficiently low so that Ostwald ripening was still the dominant growth mechanism[2] and the Sn flux created only a perturbation on Ostwald ripening due to violation of mass conservation during clustering.

The quantity of deposited material for conditions (2) and (3) was determined by *ex situ* Rutherford backscattering spectroscopy. We state the amount of metal deposit as the equivalent coverage in monolayers, where $1\,\mathrm{ML}=7.8\times10^{14}$ atoms/cm^2 for the Si(111) surface. Images of clusters were obtained *ex situ* using plan-view scanning electron microscopy (SEM).

RESULTS

We quantify the cluster ordering by first measuring the position and size of clusters from SEM micrographs. From this data, we calculate basically two distributions:

(a) *Cluster size distributions* (CSD) for size ordering. The cluster size can be specified by one linear dimension due to the equilibrium, spherically capped shape of liquid metal droplets on surfaces as present during growth for all systems in the present study. We use the plan-view diameter as this dimension. For comparison, the CSDs are plotted using the *scaled* cluster size, i.e., the cluster size relative to the average cluster size.

(b) *Nearest-neighbor distributions* (NND) for spatial ordering. The nearest-neighbor distance is defined as the center to center distance between a specified cluster and its nearest neighbor. To quantify the degree of ordering, all NND's displayed are compared with the NND's for (i) a fully ordered cluster structure and (ii) computer generated random distributions based on a random placement of clusters where the distribution is obtained from averaging a large number of simulations. All simulated distributions have the same areal density and areal coverage of clusters as the experimental distributions and they were generated with an exclusion provision against cluster perimeters overlapping.

In order to further establish the global character of ordering, and to not just sample the nearest neighbors, the NND's are supplemented by *angular distributions* for spatial orientational ordering. For this purpose, we consider the angle between the center-center lines of each cluster to its nearest- and second-nearest neighbors since the strongest interactions occur between these clusters. Angular distributions will only be shown if they do contribute details not seen on the NND's.

(1) Coalescence-dominated growth. Figure 1(a) shows an SEM plan-view image of Ga clusters on GaAs(001) after annealing of the substrate at 660 °C for 5 min. Figure 1(b) shows both the cluster size distribution obtained from the micrograph and the predicted coalescence distribution from Monte Carlo simulations carried out by Family and Meakin.[8] The distributions are plotted using logarithmic scales. Based on the agreement between the experimental data and the simulations, we conclude that the cluster growth is dominated by static coalescence, i.e., coalescence with immobile clusters. Recent coalescence events can be seen in the micrograph as cleared areas next to large clusters, i.e., where two clusters have coalesced into one larger cluster. Other regions show cleared areas with new clusters which have just nucleated. These clusters are in a transient regime and their size distribution does not yet fold back into the global cluster size distribution.[9] We therefore introduce a minimum cluster size when calculating the spatial distributions and only clusters larger than this minimum size are included in the analysis.

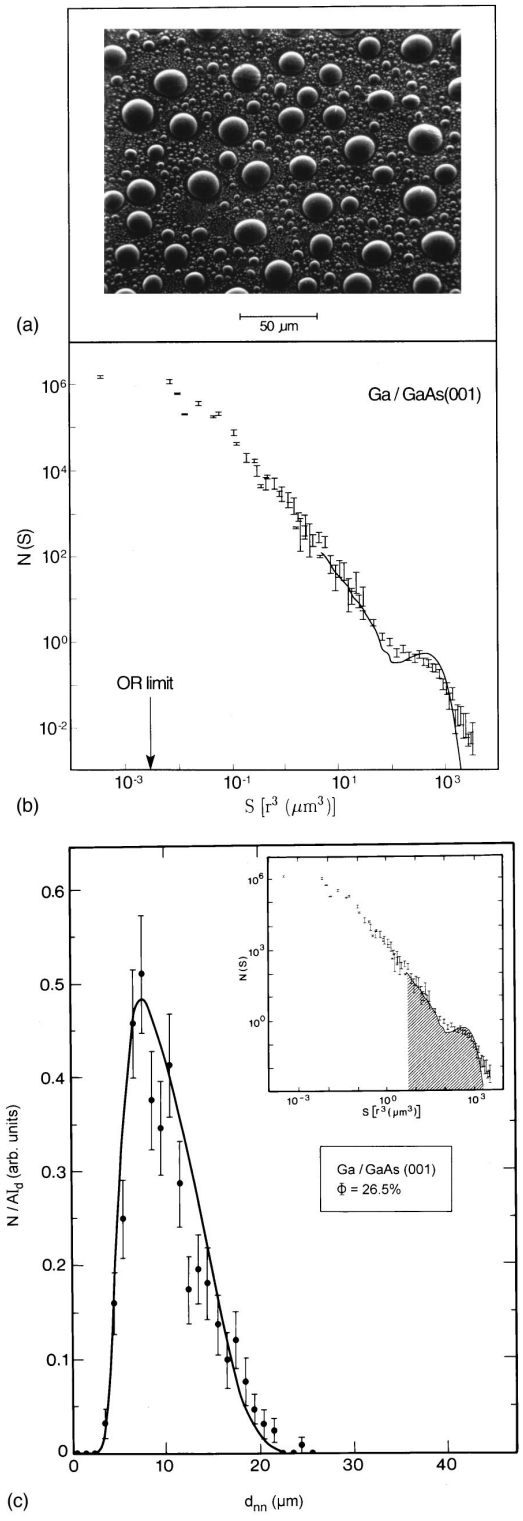

FIG. 1. (a) SEM micrograph of Ga clusters on GaAs(001). The sample was prepared by GaAs annealing at 660 °C for 5 min. (b) Cluster size distribution from the sample shown in (a) and the theoretical distribution for static coalescence (—) from Ref. 8. The mean cluster size is about five orders of magnitude larger than the typical size that results from Ostwald ripening growth (OR limit). (c) The nearest-neighbor distribution for the sample in (a). The clusters used in calculating this distribution fall within the hatched area of the cluster size distribution (inset). The areal coverage of these clusters is $\phi=26.5\%$. The nearest-neighbor experimental data are consistent with a random spatial arrangement of clusters.

This cutoff is indicated by the hatched area in the CSD in Fig. 1(c) (inset) and the areal coverage of these clusters in 26.5%. Increasing the cutoff value so that the areal coverage of the clusters was 24% provided similar results to what we present. Figure 1(c) shows the NND from the sample in Fig. 1(a). Also shown is a random NND. Based on the similarity of the plot in Fig. 1(c) to the corresponding random distribution plot, we conclude that the spatial distribution of clusters is random. The same conclusion results from a comparison of the angular distribution with a random model.

(2) Ostwald ripening-dominated growth. The results from Ostwald ripening-dominated growth are more complex since the cluster size distributions vary as a function of the surface fraction covered by clusters, i.e., the areal coverage ϕ.[10–12] We therefore examine different areal coverages for the Ostwald ripening growth regime. We experimentally study the relatively low areal coverages of about 2% for the Sn/Si(111) system, and areal coverages of about 10% for the system In/Si(111).

We begin with the low areal coverage regime. Figure 2(a) shows an SEM micrograph of Sn clusters on Si(111) with an areal coverage of 2.4%. The sample was prepared by deposition of 47 ML of Sn on a room-temperature Si substrate and post-deposit annealing at 400 °C for 10 min. The cluster size distribution for this sample is shown in Fig. 2(b) along with the Lifshitz-Slyozov (LS) distribution for the mixed geometry.[2,3] Since the LS model is an analytical mean-field model which predicts cluster size distributions exact for zero volume fractions and establishes the basis for all nonzero volume fraction models, it provides a useful comparison with the basic physical model, i.e., condition where all cluster-cluster interactions are excluded and therefore a random spatial distribution is assumed. The experimental size distribution in Fig. 2(b) has a similar functional form as the LS distribution, but note that the experimental distribution is significantly broader, indicating cluster-cluster interactions as established in finite volume fraction models.[10]

The NND distribution and angular distribution are shown in Figs. 2(c) and 2(d), respectively, along with the distributions obtained for a random placement of clusters with the same spatial density and areal coverage. The NND's for Ostwald ripening dominated growth, in contrast to the coalescence-dominated growth, are spatially more ordered as seen by the relatively narrow NND as compared to the random distribution. There are few clusters at small nearest-neighbor distances. However, as also evident from the micrograph, the clusters do not order completely. This is shown by the vertical line in Fig. 2(c) which indicates the cluster-cluster distance if all clusters would resume fully hexagonal ordered positions. The experimental angular distribution is also not in agreement with the random distribution. There is a large deficiency of clusters with small angles as compared to the random distribution which is nearly constant over the entire angular range.

The form of these Sn/Si(111) Ostwald ripening distributions after further ripening were explored by identical sample preparation except post-deposit annealing was for 120 min. This results in a final areal coverage of 1.8%. Figures 3(a)–3(c) show, respectively, an SEM micrograph, the cluster size distribution along with the LS distribution and the NND. Figure 3(c) also shows the corresponding random distribution. All of the distributions in Fig. 3, as well as the angular distribution for this sample, are similar to the ones in Fig. 2 so that, even though the spatial density of clusters decreases with increased annealing time [note the scale bars in Figs. 2(a) and 3(a)], this has very little effect on the spatial distributions.

Higher areal coverages were obtained with the In/Si(111) system. Figure 4(a) shows an SEM micrograph of a sample prepared by room-temperature deposition of 22 ML of In and post-deposit annealing at 400 °C for 40 min, resulting in an areal coverage of 10%. This high areal coverage has a different morphology than the low areal coverage regime. By visual inspection of the micrograph, the higher areal coverage has a slightly bimodal character, i.e., large clusters superimposed on a background of smaller clusters. The CSD and NND for this sample are shown in Figs. 4(b) and 4(c), respectively, along with the LS distribution and the random spatial distribution. The bimodal character of cluster sizes is seen as a small shoulder, or peak, in the CSD at relatively large cluster sizes. This bimodal character is more evident in Fig. 4(b) (inset), where the CSD is plotted using a logarithmic vertical axis. As for the lower coverages, the NND [Fig. 4(c)] and the angular distribution indicate that the spatial arrangement of clusters again is not random.

(3) Intermediate regime. The intermediate regime was explored for the system Sn/Si(111). Sn was deposited at a rate of 1 Å/min for 120 min on Si(111) held at a temperature of 360 °C. An SEM micrograph of this sample is shown in Fig. 5(a) and shows a propensity towards the grouping of clusters into pairs. This type of grouping is not observed for Ostwald ripening systems obeying mass conservation (micrographs in Figs. 2, 3, and 4). The CSD from this micrograph (and others) is shown in Fig. 5(b) along with the LS distribution. The NND is shown in Fig. 5(c) along with the corresponding random distribution. The CSD is surprisingly narrower than those obtained from samples obeying the mass conservation constraints of LS theory. While the tendency for the pairing of clusters seems to indicate a spatial ordering, it is actually disordering. This is seen by the NND, which has significantly broadened (compared to those obtained with Ostwald ripening) and is close to a random distribution. Thus the ''grouping'' is providing the small nearest-neighbor distances that occur for random configurations. The angular distribution is also in agreement with a random distribution.

We summarize the ordering from the different growth regimes in Table I where we include (i) the clustering system, (ii) the dominant growth mechanism, (iii) the areal coverage, (iv) the standard deviation of the cluster size distribution relative to the average cluster size, (v) the standard deviation of the NND relative to the average nearest-neighbor distance, and (vi) the product of the standard deviations of the CSD and the NND for each sample. The standard deviation of the LS NND was obtained by computer simulation where clusters of zero size were randomly distributed on a surface. The product of the two standard deviations provides a measure of the degree of double ordering (both spatial and size). As this number decreases, the degree of ordering increases.

Table I shows the following:

(1) The theoretical limit of Ostwald ripening dominated growth given by LS theory, has a narrow CSD ($\sigma = 0.157$) and a random NND (the randomness is an inherent part of

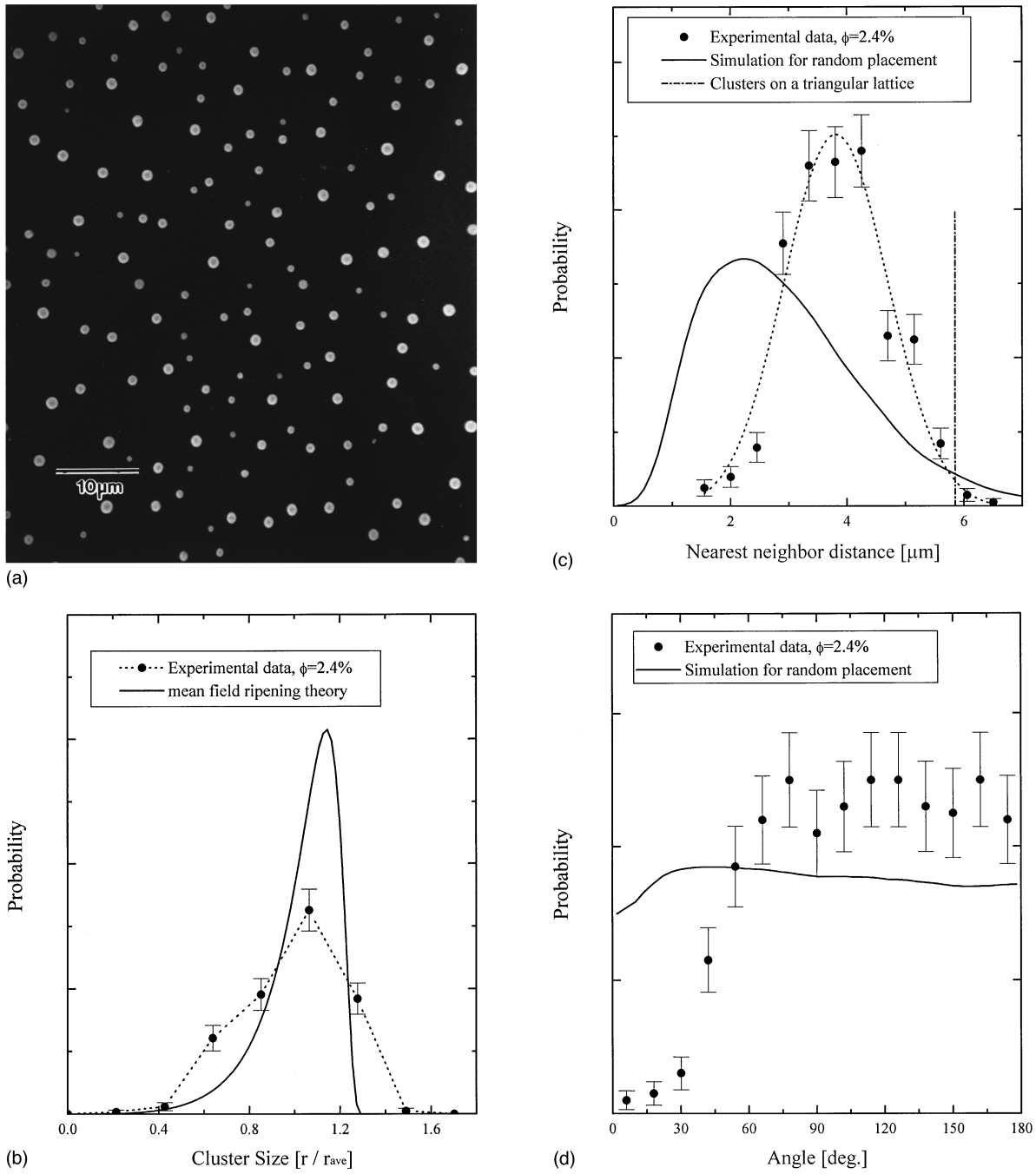

FIG. 2. (a) SEM micrograph of Sn clusters on Si(111). The sample was prepared by Sn deposition on room-temperature Si and post-deposit annealing at 400 °C for 10 min. The resulting areal coverage of clusters is $\phi = 2.4\%$. (b) The cluster size distribution from the sample in (a) and the mean-field Ostwald ripening distribution from Ref. 2. The experimental distribution is broader than the theoretical distribution. (c) The nearest-neighbor distribution from the sample in (a). The experimental distribution is more ordered than the distribution for a random spatial arrangement of clusters. (d) The angular distribution from the sample in (a). The experimental distribution has fewer clusters subtending small angles than the distribution for a random placement of clusters.

the mean-field nature of the theory[2,3]).

(2) While still maintaining Ostwald ripening conditions, i.e., mass conservation, but increasing the areal fraction, ϕ, of clusters the CSD becomes more disordered (broader) but, at the same time, the NND becomes more ordered (narrower). The product of the standard deviations of the CSD and the NND, is smaller than the LS limit and indicates an overall increase in the ordering when finite ϕ effects are included.

(3) If the areal coverage is large enough (e.g., 10%) partial ordering is still occurring, however, the degree of ordering is less for the higher coverages.

(4) As mass conservation is violated (by allowing for a small external flux) we observe at finite areal fraction ϕ that the size distribution is only slightly broader than the LS prediction, i.e., it is significantly narrower than experimental distributions at the same ϕ grown under mass conservation as discussed above.[11] The NND on the other hand is nearly

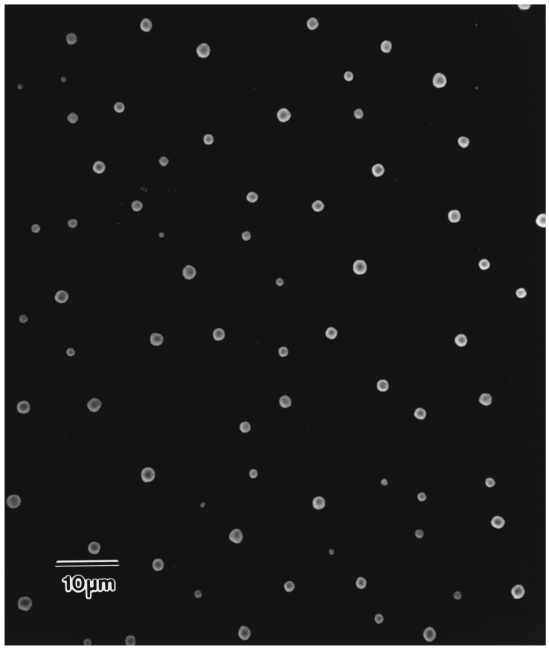

(a)

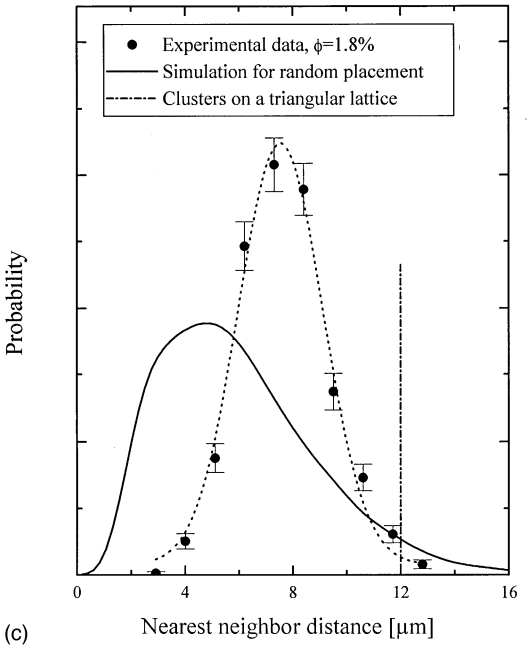

(c)

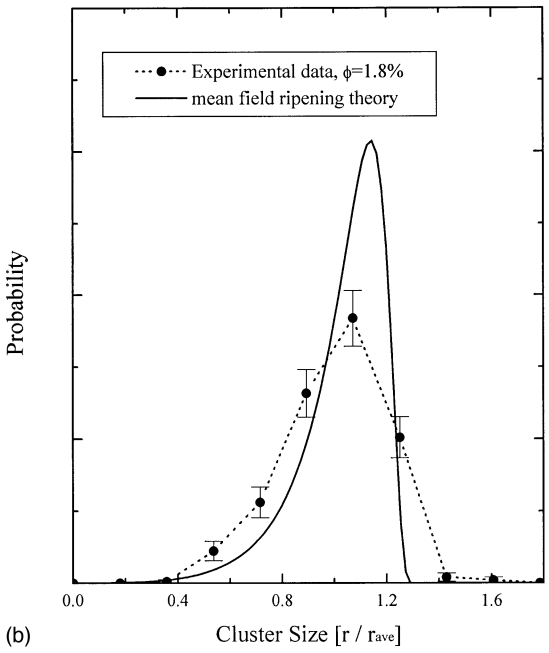

(b)

FIG. 3. (a) SEM micrograph of Sn clusters on Si(111). This sample was prepared by room-temperature deposition of Sn on Si and post-deposit annealing at 400 °C for 120 min. The resulting areal coverage of clusters is $\phi = 1.8\%$. (b) The cluster size distribution from the sample in (a) and the mean-field Ostwald ripening distribution from Ref. 2. The experimental distribution is broader than the theoretical distribution. (c) The nearest-neighbor distribution from the sample in (a). The experimental distribution is more ordered than the distribution for a random spatial arrangement of clusters.

random. Thus, with a small flux, the σ values are nearly the LS values.

(5) At the limit of coalescence-dominated growth, the CSD is very disordered (i.e., broad) and the NND is disordered (consistent with a random distribution).

In addition to the ordering as seen by the NND and the CSD, angular ''ordering'' is observed for Ostwald ripening conditions at finite ϕ as shown in Fig. 2(d). This ordering is seen by the exclusion of small angles when compared to the random distribution, and the probability of having certain angles in the distribution only becomes constant at angles greater than about 50°–60°. This exclusion at low angles is related to the distance ordering observed, i.e., since the NND are quite narrow, the probability of three clusters subtending a small angle will only become significant when the three clusters form an equilateral triangle with sides equal to the minimum distance in the NND. Therefore, the angular distribution should start to reach a maximum at angles of 60°.

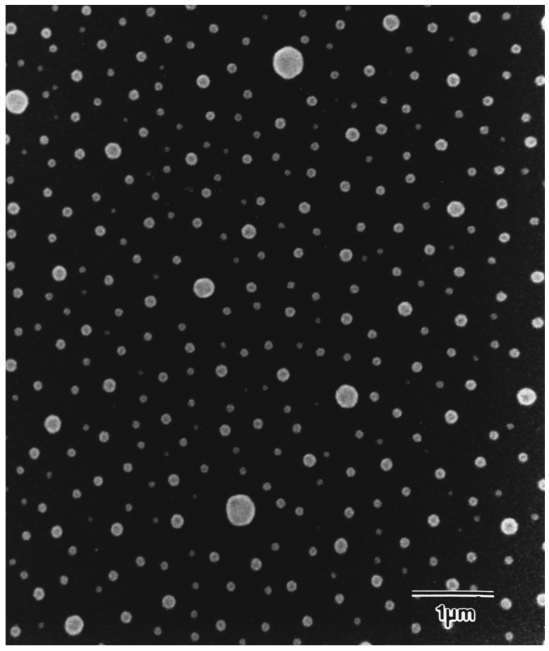

(a)

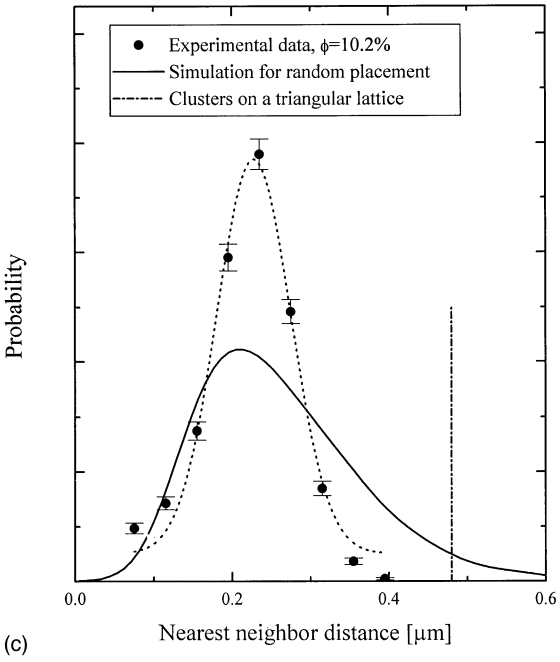

(c)

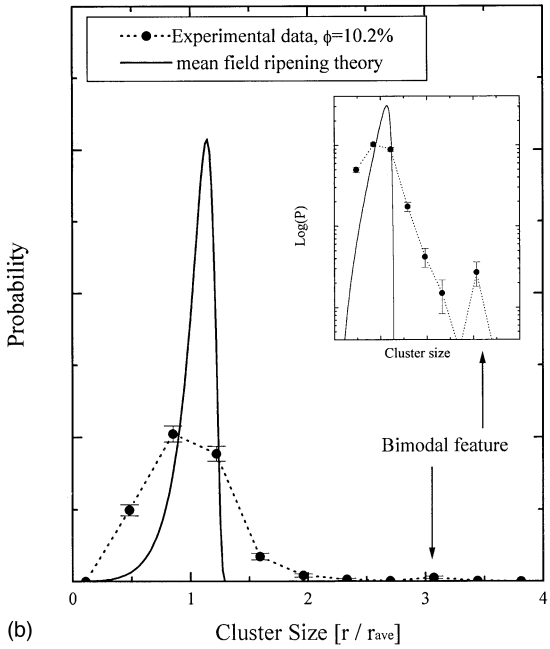

(b)

FIG. 4. (a) SEM micrograph of In clusters on Si(111). The sample was prepared by room-temperature deposition of In on Si and post-deposit annealing at 400 °C for 10 min. The resulting areal coverage is $\phi = 10.2\%$. (b) Cluster size distribution for the sample in (a) along with the theoretical Ostwald ripening distribution from Ref. 2. The data are displayed with a linear vertical axis (main plot) and a logarithmic vertical axis (inset). A bimodal character of the distribution is seen most easily in the logarithmic representation. (c) The nearest-neighbor distribution from the sample in (a). The experimental distribution of clusters on the surface is not random. Note, however, that this distribution is not as ordered as the Ostwald ripening distributions in Figs. 2 and 3 (see Table I).

DISCUSSION

Ordering in clustering on surfaces during different growth regimes can be established in (1) size ordering of the cluster size distribution, and (2) spatial ordering in the nearest-neighbor distribution and the angular distribution. We now discuss the possible mechanisms for ordering in light of our experimental data.

Theoretical concepts for ordering in the literature. (i) One potential mechanism for spatial ordering is heterogeneous nucleation of clusters in the initial stages of the phase separation. We rule out this possibility since the spatial density of clusters in the nucleation stage is many orders of magnitude larger than the spatial densities of clusters observed after Ostwald ripening.[13] Therefore, any ordering during nucleation would not survive a random ''extinction'' process in the Ostwald ripening stages of growth and so any

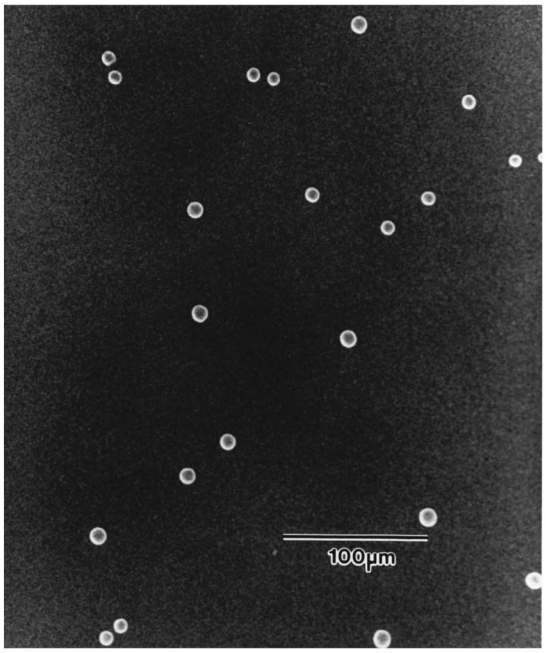

(a)

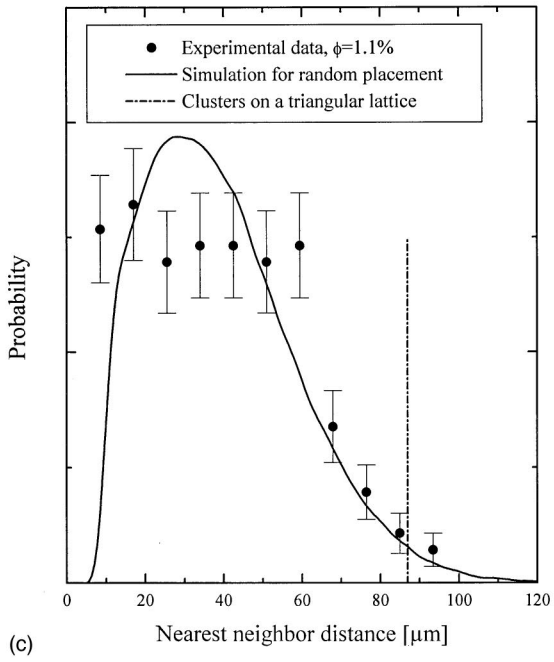

(c)

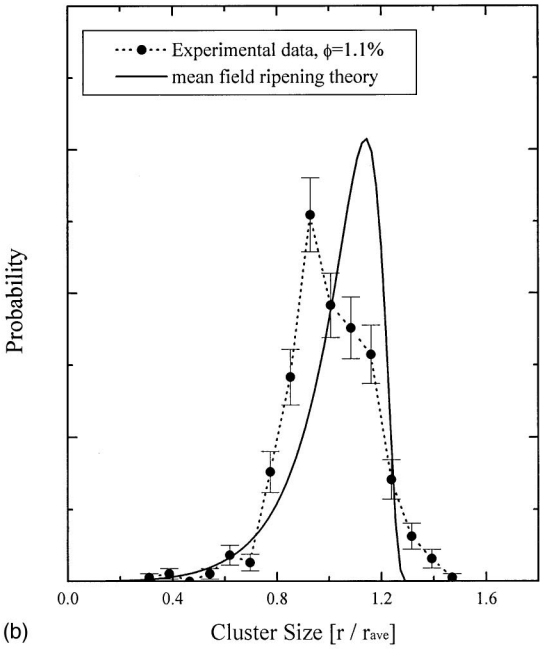

(b)

FIG. 5. (a) SEM micrograph of Sn clusters on Si(111). The sample was prepared by deposition of Sn (at a rate of 1 Å/min) on Si held at a temperature of 400 °C. The deposition lasted for 120 min. The resulting areal coverage is $\phi = 1.1\%$. Ripening conditions are not obeyed since the mass of the clustered material is not conserved during growth. (b) Cluster size distribution for the sample in (a) along with the theoretical Ostwald ripening distribution from Ref. 2. The experimental distribution is in better agreement with mean field Ostwald ripening theory than the samples in Figs. 2, 3, and 4 (see Table I). (c) The nearest-neighbor distribution from the sample in (a). The experimental distribution of clusters on the surface is in agreement with a random distribution.

ordering must at least be sustained in the later stages of growth. All other models in literature require (i) mobile clusters and (ii) attractive or repulsive forces between clusters beyond the capillarity effect introduced by Liftshitz and Slyozov.

(ii) Long-range repulsive interactions between coarsening particles were studied by Sagui and Desai,[14] introducing these interactions through a power-law ansatz. The particles then tend to order through cluster motion in response to the repulsive force into a regular hexagonal lattice with both distance and orientational ordering. The clustering systems used in the present study do not lend themselves well to such long-range repulsive forces. Electrostatic and magnetic forces considered in Ref. 14 do not occur. Elastic interac-

TABLE I. Summary of the experimental data. Shown are the clustering system, the growth regime, the areal coverage of clusters, the standard deviation of the cluster size distribution scaled to the average cluster size (σ_{CSD}) which is a measure of the size ordering, the standard deviation of the nearest-neighbor distribution scaled to the average nearest-neighbor distance (σ_{NND}) which is a measure of the spatial ordering, and the product of the two standard deviations which is a measure of the total ordering.

System	Growth mechanism	Areal coverage (%)	σ_{CSD}	σ_{NND}	$\sigma_{CSD}*\sigma_{NND}$
Theoretical	LS ripening	0	0.157	0.54	0.085
Sn/Si(111)	ripening	1.8	0.20 ± 0.02	0.22 ± 0.02	0.044 ± 0.008
Sn/Si(111)	ripening	2.4	0.23 ± 0.02	0.23 ± 0.02	0.053 ± 0.009
In/Si(111)	ripening	10.2	0.32 ± 0.01	0.27 ± 0.01	0.086 ± 0.009
Sn/Si(111)	intermediate	1.1	0.17 ± 0.01	0.54 ± 0.02	0.092 ± 0.009
Ga/GaAs(001)	coalescence	26.5	N/A	0.39 ± 0.02	

tions between clusters (mediated by the substrate) are perhaps the most likely candidate. However, most models that include elastic interactions recognize that the effects are only prominent for solid-solid systems[15] and the present experiments are under conditions for which the clusters are liquid during growth. We believe therefore that elastic interactions would be too weak to support ordering for clusters several micrometer apart from each other.

(iii) Attractive forces due to diffusive interactions between particles were proposed by Voorhees and Schaefer.[16] In their study these forces result in particle motion to unoccupied regions within the matrix which leads to a more uniform spatial distribution. Such particle motion should eventually result in particle arrangement on a regular lattice and in addition to distance ordering, special angles should become prominent in the angular distributions. This type of ordering would increase with elapsed time during cluster growth since clusters have more time to achieve ordered positions. This increase in distance and orientational ordering during cluster evolution are not observed in the present study for the Sn/Si(111) system. We conclude therefore that the type of cluster interactions proposed in Ref. 16 are not dominant in our ordering processes.

Local ripening and screening. We propose the mechanism responsible for distance ordering is *local ripening*. This mechanism results from the local diffusive interactions between two sufficiently close particles.[17] The interaction induces the smaller of the two to decompose into the larger, regardless of whether the smaller of the two is large enough so that it would otherwise grow based on the LS mean-field theory. This interaction, while diffusive in nature (as is the interaction introduced by Voorhees and Schaefer[16]), does not require the motion of particles to create spatial ordering.

For a detailed description of local ripening and ordering that follows, we use plots of the supersaturation, c, of the adatom phase on the surface in the vicinity of clusters. We first begin with the LS mean-field theory as shown in Fig. 6(a). This theory can be viewed as examining an individual cluster that evolves in the average supersaturation that is created by the other clusters on the surface. For an isolated three-dimensional cluster on a surface, the solution of the quasistatic diffusion equation subject to the Gibbs-Thomson boundary condition at the cluster edge results in a $c(x)$ profile that increases logarithmically with distance from the cluster. This profile levels off to the average level c_0 at a given distance, or ''screening length,'' from the cluster.[4,18] The placement of clusters on the surface is random as this is an inherent part of the mean-field nature of the theory.

Actual Ostwald ripening experiments do not strictly obey the mean-field approximations and cluster-cluster interactions occur through local diffusive interactions. Once these are included, the evolution of a cluster depends on its local environment. For example, two clusters that are sufficiently close together, i.e., much closer than the screening length, create a local gradient in the supersaturation that is largest in the region between the two clusters [Fig. 6(b)]. This results in the smaller of the two clusters to decompose into the larger. Assuming the smaller of the two clusters is sufficiently large so that it should grow based on the mean-field theory, this local interaction has two effects: (i) it reduces the possibility of two clusters being in close proximity and this narrows the NND and creates a partial spatial ordering of the clusters, i.e., the distribution is no longer random, and (ii) it broadens the CSD since the larger of the two clusters gains more material and grows larger than it would based on mean-field predictions, i.e., it moves farther to the right in the distribution and results in broadening. Therefore, local ripening both broadens the CSD and narrows the NND.

The next progression in the description imposes a small external flux during Ostwald ripening dominated growth. This flux tends to increase the average supersaturation level on the surface. The supersaturation level at the cluster boundary, however, is still given by the Gibbs-Thomson boundary condition. Therefore, with a small flux, the $c(x)$ profile between two clusters would appear as in Figs. 6(c) and 6(d) for increasing levels of flux, respectively. Under a relatively small flux, the $c(x)$ level only increases near the mid-region between the two clusters. Therefore, provided the supersaturation level stays well below the nucleation threshold, the dominant effect of the flux is to screen out local ripening and allow two clusters in close proximity to survive. Therefore, one begins to recover LS conditions (except for the small violation of mass conservation) and cluster size distributions and spatial distributions are in close agreement with the LS theory.

As the external flux is further increased, the coalescence regime is approached. This requires that the external flux is large enough so that the supersaturation reaches the level

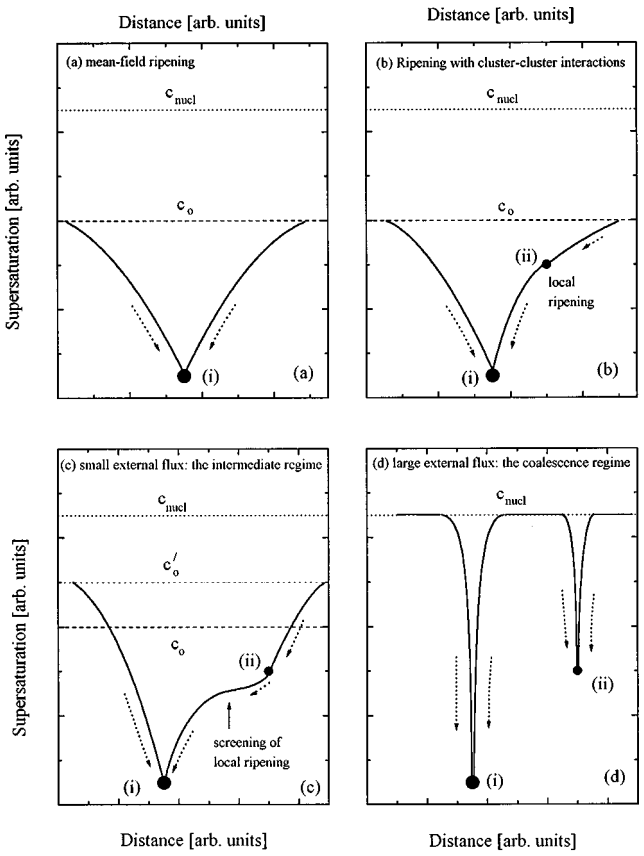

FIG. 6. A schematic representation of local ripening showing the free adatom concentration, c, as a function of a distance from a cluster. c_0 is the average concentration on the surface, c_{nucl} is the threshold concentration for nucleation. (a) Mean-field theory where local ripening is not considered. The cluster (solid circle), is larger than the average cluster size and therefore gains material from the supersaturation. (b) Local ripening with no external flux of material. The cluster (ii) would normally grow based on mean-field theory, but instead decomposes into cluster (i). This results in a decreased probability for small nearest-neighbor distances. (c) An external flux increases the average concentration level to c_0'. The local increase in the concentration between the two clusters ''screens out'' local ripening and the two cluster do not interact. The cluster (ii) now grows instead of decomposing. If the flux is sufficiently small so the supersaturation does not reach the nucleation threshold concentration, then mean-field conditions can be nearly recovered. (d) A large external flux increases the average concentration between clusters up to c_{nucl} and new clusters continually nucleate. Local ripening is completely suppressed between all clusters, as is Ostwald ripening in general. This describes the coalescence growth regime.

required for nucleation of new clusters and complete screening of ripening [Fig. 6(d)]. At this point, new clusters continually nucleate and all clusters grow independent of their size. There is no local ripening since the effects of one cluster on another are screened out by the external flux. Thus one obtains a broad CSD and a broad, i.e., random, NND.

The spatial ordering that occurs during Ostwald ripening suggests that local ripening can be thought of as an ''effective force'' between clusters. An analytical form describing such a force has, to our knowledge, not been formulated. This type of force is attractive when considering the transfer of material between two clusters undergoing local ripening. This is due to the accelerated transfer of material, as compared to LS ripening, from a large and small cluster in close proximity on a surface. However, this force can also be thought of as a repulsive one when considering the NND's shown in Figs. 2(c), 3(c), and 4(c). The random distributions result when no interactions occur, and the distribution for a fully ordered triangular lattice of clusters would occur with repulsive interactions between clusters as described by Sagui and Desai.[14] The experimental distributions are shifted away from the random distributions and towards the distribution for the triangular lattice and implies a repulsive force between clusters (a shift of the distributions instead to the left of the random distributions would imply an attractive force).

The effects of early stage coalescence. Finally, we discuss the size and spatial ordering as the effects of local ripening are increased (i.e., larger ϕ). We expect the that spatial distribution would become more ordered, however this is not the case as the In/Si(111) system, with an areal coverage of 10%, has a broader NND than the 1.8% coverage Sn/Si(111). The reason for this observation is that the In/Si(111) sample not only has a higher areal fraction but at the same time represents in terms of a ripening evolution an early stage rather than late stage morphology, as considered for the Sn/Si systems above.

Late stage Ostwald ripening follows an initial nucleation phase and a transitional regime where nucleation ceases and the cluster size distribution approaches the narrow, unimodal late stage LS distribution. For the transition from the nucleation stage to initial cluster growth, it is well established[13] that coalescence is a major effect in reducing the supersaturation levels and thus terminating further nucleation. The mechanism of coalescence during this stage is the same as discussed above as a late stage process, except that it will occur as a transient process under mass conservation, ceasing fast as clusters grow and thus become on average spatially more separated. Like in the late stage model, coalescence will lead to a tendency of the cluster size distribution toward a bimodal character or, at least to a tail toward larger cluster sizes, due to sudden merger of two or more clusters. Naturally, at larger areal cluster coverages this transient coalescence stage preceding late stage Ostwald ripening will prevail longer as clusters are spatially much closer to each other increasing the likelihood of cluster-cluster contact.

This effect is visible for our In/Si(111) sample with a final areal coverage of 10%. The observed weak bimodality is attributable to the effects of early stage coalescence. The transient coalescence contribution tends also to randomize the spatial distribution as seen in the first part of our study for the system Ga/GaAs(001). Therefore, spatial ordering cannot necessarily be increased by increasing ϕ, unless at the same time the effects of early stage coalescence could be reduced.

CONCLUSIONS

Local ripening interactions and screening of these interactions by an external flux during cluster growth on surfaces play important roles in the achievement of partial spatial ordering and size ordering of the clusters. With no external flux, local ripening (i) broadens the cluster size distribution

relative to the LS distribution and (ii) narrows the nearest-neighbor distributions compared to random distributions. Thus partially ordered structures (spatial ordering) can be obtained during Ostwald ripening with interactions that do not require the motion of individual clusters or direct interactions with the substrate. The local ripening interactions can be screened out by a small external flux and without local ripening, LS clusters size distributions and random nearest-neighbor distributions are nearly obtained. When the external flux is sufficiently large, Ostwald ripening is suppressed, nucleation of new clusters occurs, coalescence events dominate the cluster morphologies and broad cluster size distributions, and random nearest-neighbor distributions result.

ACKNOWLEDGMENT

This work was carried out with funding from the Natural Sciences and Engineering Research Council of Canada.

[1] D. S. L. Mui, D. Leonard, L. A. Coldren, and P. M. Petroff, Appl. Phys. Lett. **66**, 1620 (1995); S. Jeppesen, M. S. Miller, D. Hessman, B. Kowalski, I. Maximov, and L. Samuelson, *ibid.* **68**, 2228 (1996); M. Kitamura, N. Nishioka, J. Oshinowo, and Y. Arakawa, *ibid.* **66**, 3663 (1995); A. Ponchet, A. Le Corre, H. L'Haridon, B. Lambert, and S. Salaün, *ibid.* **67**, 1851 (1995).

[2] M. Zinke-Allmang, L. C. Feldman, and M. H. Grabow, Surf. Sci. Rep. **16**, 377 (1992).

[3] I. M. Lifshitz and V. V. Slyozov, Zh. Eksp. Teor. Fiz. **35**, 479 (1958) [Sov. Phys. JETP **35**, 331 (1959)]; J. Chem. Phys. **19**, 35 (1961).

[4] B. K. Chakraverty, J. Chem. Phys. Solids **28**, 2401 (1967).

[5] A. Ishizaka and Y. Shiraki, J. Electrochem. Soc. **133**, 666 (1986).

[6] T. D. Lowes (private communication); T. D. Lowes and M. Zinke-Allmang, J. Appl. Phys. **73**, 4937 (1993).

[7] M. Zinke-Allmang, L. C. Feldman, and W. van Saarloos, Phys. Rev. Lett. **68**, 2358 (1992).

[8] F. Family and P. Meakin, Phys. Rev. Lett. **61**, 428 (1988).

[9] M. Zinke-Allmang, S. Puddephatt, and T. D. Lowes, in *Epitaxial Growth Processes*, edited by C. J. Palmstrøm and M. C. Tamargo (SPIE, Bellingham, Washington, 1994), Vol. 2140, p. 36.

[10] Y. Enomoto, M. Tokuyama, and K. Kawasaki, Acta Metall. **34**, 2119 (1986); P. W. Voorhees and M. E. Glicksman, *ibid.* **32**, 2013 (1984); J. A. Marqusee, J. Chem. Phys. **81**, 976 (1984).

[11] G. R. Carlow and M. Zinke-Allmang, Surf. Sci. **328**, 311 (1995).

[12] R. Barel, Y. Mai, G. R. Carlow, and M. Zinke-Allmang, Appl. Surf. Sci. **104/105**, 669 (1996).

[13] J. A. Venables, Philos. Mag. **7**, 697 (1973); M. Hanbücken, M. Futamoto, and J. A. Venables, Surf. Sci. **147**, 433 (1984).

[14] C. Sagui and R. C. Desai, Phys. Rev. Lett. **74**, 1119 (1993).

[15] K. Binder, Phys. Rev. B **15**, 4925 (1977).

[16] P. W. Voorhees and R. J. Schaefer, Acta Metall. **35**, 327 (1987).

[17] J. P. Hirth, J. Cryst. Growth **17**, 63 (1972).

[18] M. Zinke-Allmang, S. Yu. Krylov, and G. R. Carlow, Scanning Microsc. (to be published).